



INTERNATIONAL APPLICATION PUBLISHED UNDER THE PATENT COOPERATION TREATY (PCT)

(51) International Patent Classification ⁶ : A61K 51/00	A2	(11) International Publication Number: WO 99/00150 (43) International Publication Date: 7 January 1999 (07.01.99)
(21) International Application Number: PCT/US98/13398 (22) International Filing Date: 26 June 1998 (26.06.98) (30) Priority Data: 60/051,065 27 June 1997 (27.06.97) US (71) Applicant (for all designated States except US): REGENTS OF THE UNIVERSITY OF CALIFORNIA [US/US]; 22nd floor, 300 Lakeside Drive, Oakland, CA 94612-3550 (US). (72) Inventor; and (75) Inventor/Applicant (for US only): PARDRIDGE, William, M. [US/US]; 1180 Tellem Drive, Pacific Palisades, CA 90272 (US). (74) Agent: KONDZELLA, Michael, A.; Oppenheimer Wolff & Donnelly LLP, Suite 3800, 2029 Century Park East, Los Angeles, CA 90067-3024 (US).		(81) Designated States: AU, CA, JP, US, European patent (AT, BE, CH, CY, DE, DK, ES, FI, FR, GB, GR, IE, IT, LU, MC, NL, PT, SE). Published <i>Without international search report and to be republished upon receipt of that report.</i>
(54) Title: DRUG TARGETING OF A PEPTIDE RADIOPHARMACEUTICAL THROUGH THE PRIMATE BLOOD-BRAIN BARRIER IN VIVO WITH A MONOCLONAL ANTIBODY TO THE HUMAN INSULIN RECEPTOR (57) Abstract <p>[¹²⁵I]-Aβ¹⁻⁴⁰ was mono-biotinylated and conjugated to a blood-brain barrier drug delivery and brain targeting system comprised of a complex of the 83-14 monoclonal antibody (MAb) to the human insulin receptor, which is tagged with streptavidin (SA) to produce a marked increase in rhesus monkey brain uptake of the [¹²⁵I]-bio-Aβ¹⁻⁴⁰ at 3 hours following intravenous injection compared to no measurable brain uptake of [¹²⁵I]-bio-Aβ¹⁻⁴⁰ in the absence of a BBB drug.</p>		

FOR THE PURPOSES OF INFORMATION ONLY

Codes used to identify States party to the PCT on the front pages of pamphlets publishing international applications under the PCT.

AL	Albania	ES	Spain	LS	Lesotho	SI	Slovenia
AM	Armenia	FI	Finland	LT	Lithuania	SK	Slovakia
AT	Austria	FR	France	LU	Luxembourg	SN	Senegal
AU	Australia	GA	Gabon	LV	Latvia	SZ	Swaziland
AZ	Azerbaijan	GB	United Kingdom	MC	Monaco	TD	Chad
BA	Bosnia and Herzegovina	GE	Georgia	MD	Republic of Moldova	TG	Togo
BB	Barbados	GH	Ghana	MG	Madagascar	TJ	Tajikistan
BE	Belgium	GN	Guinea	MK	The former Yugoslav Republic of Macedonia	TM	Turkmenistan
BF	Burkina Faso	GR	Greece	ML	Mali	TR	Turkey
BG	Bulgaria	HU	Hungary	MN	Mongolia	TT	Trinidad and Tobago
BJ	Benin	IE	Ireland	MR	Mauritania	UA	Ukraine
BR	Brazil	IL	Israel	MW	Malawi	UG	Uganda
BY	Belarus	IS	Iceland	MX	Mexico	US	United States of America
CA	Canada	IT	Italy	NE	Niger	UZ	Uzbekistan
CF	Central African Republic	JP	Japan	NL	Netherlands	VN	Viet Nam
CG	Congo	KE	Kenya	NO	Norway	YU	Yugoslavia
CH	Switzerland	KG	Kyrgyzstan	NZ	New Zealand	ZW	Zimbabwe
CI	Côte d'Ivoire	KP	Democratic People's Republic of Korea	PL	Poland		
CM	Cameroon	KR	Republic of Korea	PT	Portugal		
CN	China	KZ	Kazakstan	RO	Romania		
CU	Cuba	LC	Saint Lucia	RU	Russian Federation		
CZ	Czech Republic	LI	Liechtenstein	SD	Sudan		
DE	Germany	LK	Sri Lanka	SE	Sweden		
DK	Denmark	LR	Liberia	SG	Singapore		
EE	Estonia						

**DRUG TARGETING OF A PEPTIDE RADIOPHARMACEUTICAL THROUGH
THE PRIMATE BLOOD-BRAIN BARRIER IN VIVO WITH A
MONOCLONAL ANTIBODY TO THE HUMAN INSULIN RECEPTOR**

BACKGROUND OF THE INVENTION

The present invention relates generally to the introduction of radiolabeled peptide pharmaceutical agents into the brain by transcytosis across the blood-brain barrier.

Peptide radiopharmaceuticals have potential for diagnostic imaging. The somatostatin receptor is overexpressed in certain neuroendocrine tumors, as well as brain tumors, such as meningiomas or gliomas and [^{125}I]- or [^{111}In]-labeled octreotide, a somatostatin peptide analog, has been used to image these tumors. Owing to the small size of the peptide radiopharmaceutical, octreotide readily crosses the porous capillaries perfusing tumors in the periphery, or certain brain tumors, such as meningiomas, which lack a blood-brain barrier (BBB). However, well-differentiated gliomas, which also overexpress somatostatin receptors, have an intact BBB, and it is not possible to image these tumors with octreotide, since this peptide does not cross the BBB in vivo.

In addition to tumors, it should also be possible to image other medical disorders with peptide radiopharmaceuticals, such as amyloid. The deposition of amyloid in brain of Alzheimer's Disease (AD) correlates with the degree of dementia in this disorder. Extracellular AD amyloid is comprised of two types: senile (neuritic) plaque and vascular amyloid. Both types of amyloid in AD are comprised of a 43 amino acid amyloidotic peptide, designated $\text{A}\beta^{1-43}$, as well as $\text{A}\beta^{1-42}$ forms, which are produced from the abnormal proteolysis of a normal cellular protein, the amyloid peptide precursor.

The $\text{A}\beta$ amyloid of tissue sections of AD autopsy brain can be identified with dyes, such as Congo Red, or with antibodies directed against certain epitopes of the $\text{A}\beta^{1-42/43}$ peptide. However the $\text{A}\beta$ amyloid of AD sections may also be identified in vitro by autoradiography with [^{125}I]- $\text{A}\beta^{1-40}$, a peptide which contains the first 40 amino acids of the $\text{A}\beta^{1-42/43}$ peptide, and which deposits with high affinity onto pre-existing $\text{A}\beta$ amyloid. Therefore, radiolabeled $\text{A}\beta^{1-40}$ is a potential peptide radiopharmaceutical that could be used for neurodiagnostic quantitation of the $\text{A}\beta$ amyloid burden in AD brain of living subjects using standard external detection methodologies, such as single photon emission computed tomography (SPECT) or positron emission tomography (PET). However, [^{125}I]- $\text{A}\beta^{1-40}$ does not cross the BBB in rats unless a vector mediated BBB drug delivery system is used. $\text{A}\beta$ amyloid does not deposit in the brain of aged rats, but $\text{A}\beta$ amyloid

does form in the brain of New World primates, such as the aged (15-20 years) squirrel monkey in the form of vascular amyloid, and A β amyloid is produced in the brain of Old World primates, such as the aged (27-30 years) rhesus monkey in neuritic plaque form.

It is an object of the present invention to prepare a radiolabeled peptide pharmaceutical conjugated to a BBB delivery system.

It is another object of this invention to deposit radiolabeled truncated analogs of A β ¹⁻⁴³ on amyloid plaques in AD brain tissue without impairment following conjugation to a BBB delivery system.

Another object of the invention is to enhance the brain uptake of a peptide radio-pharmaceutical with the use of a BBB drug targeting system.

SUMMARY OF THE INVENTION

Radiolabeled truncated analogs of A β ¹⁻⁴³ conjugated to a BBB drug delivery system are enabled to enter the brain from blood to a high degree, which allows for imaging amyloid plaques in AD brain tissue following systemic (intravenous) injection. Radiolabeling can be accomplished using ¹²⁵I, ¹¹¹In, or ^{99m}Tc, for example. A highly effective drug delivery system is 83-14 HIRMAb, the 83-14 monoclonal antibody to the human insulin receptor, which can be conjugated to radiolabeled truncated analogs of A β ¹⁻⁴³ by means of avidin-biotin technology, polyethyleneglycol, or other polymeric linking agents.

BRIEF DESCRIPTION OF THE DRAWINGS

Figure 1: Gel filtration (left panel, A and B) and immobilized iminobiotin affinity (right panel, C and D) chromatography of MAb 8314-streptavidin (8314-SA) conjugate. The fraction size of the gel filtration was 3 mL, and the fraction size in the affinity chromatography was 0.5 mL.

Figure 2: HILC elution and TCA precipitability percentage of bio-A β ¹⁻⁴⁰ after radiolabeling with [¹²⁵I]. The fraction size was 1 mL. The percentage of acetonitrile for each step elution is shown.

Figure 3: Gel filtration HPLC profile of [¹²⁵I]-bio-A β ¹⁻⁴⁰ (top) and [¹²⁵I]-bio-A β ¹⁻⁴⁰/8314-SA conjugate (bottom). The salt volume of the gel filtration HPLC column is 14.3

mL, while the elution volume of [125 I]-bio-A β^{1-40} was 12 mL, and that of [125 I]-bio-A β^{1-40} /8314-SA was 6 mL.

Figure 4: Time-course of 0.5 nM 8314-SA binding to human brain capillary preparation in the absence (closed circles) or the presence (open circles) of the 10 μ g/mL 8314 MAb. The tracer used in this radio-receptor assay was [3 H]-biotin (1nM), which binds to the 8314-SA conjugate with a high affinity. No competition of [3 H]-biotin/8314-SA conjugate uptake by the capillaries was observed with 10 μ g/mL mouse IgG_{2a}, the isotype control for the 83-14 MAb. The capillary uptake of [3 H]-biotin bound to streptavidin alone was <2%. Data are means of duplicates that varied <10%.

Figure 5: Time-course of [125 I]-bio-A β^{1-40} (0.23 nM) binding to human brain capillary preparation, in the presence of (a) buffer, (b) 0.5 nM 8314-SA, or (c) 0.5 nM 8314-SA plus 10 μ g/mL unconjugated 8314 MAb. Data are mean \pm SE (n=3).

Figure 6: Emulsion autoradiography showing the binding of [125 I]-bio-A β^{1-40} (A) or [125 I]-bio-A β^{1-40} /8314-SA conjugate (B) to amyloid plaques of frozen section of human AD brain under brightfield microscopy. Magnification bar is 23 μ m.

Figure 7: (A) Plasma profile of either unconjugated [125 I]-bio-A β^{1-40} (open circles) or the [125 I]-bio-A β^{1-40} /8314-SA conjugate (closed circles) after an i.v. dose of 300 μ Ci per monkey. (B) Time-course of the percent of plasma radioactivity that was precipitable with TCA after the i.v. injection.

Figure 8: Brain volume of distribution (V_D) of either [125 I]-bio-A β^{1-40} or the [125 I]-bio-A β^{1-40} /8314-SA conjugate at 3, 24, or 48 hours after i.v. injection to rhesus monkeys. The filled bars represent the V_D values of gray matter, while the open bars represent those of white matter of the monkey brains. Data are mean \pm SE (n=3).

Figure 9: Phosphorimager scans for left or right cerebral hemisphere in two different rhesus monkeys. The images in panel A represent the brain uptake 3 hours following intravenous injection of 300 μ Ci of unconjugated [125 I]-bio-A β^{1-40} . The images in the right hand panel (B) represent the brain uptake 3 hours after intravenous injection of [125 I]-bio-A β^{1-40} conjugated to 8314/streptavidin. Images for the left and right occipital lobes are shown.

Figure 10: Phosphorimages representing the brain uptake of [125 I]-bio-A β^{1-40} conjugated to the 8314/streptavidin delivery system at 3 hours (A), 24 hours (B), and 48 hours (C) following an intravenous injection of 300 μ Ci per rhesus monkey. Three different monkeys were used for these studies; one each for the measurements at 3, 24, and 48 hours, respectively. The images on the left side of the figure represent the brain uptake in the left occipital lobe, and the images on the right represent the brain uptake in the right occipital lobe.

Figure 11: Scheme depicting the multifunctionality and three domains of the peptide radiopharmaceutical conjugated to the blood-brain barrier (BBB) delivery system. The imaging agent is comprised of amyloid binding domain, a linker domain, and a BBB transport domain, the latter constituted by the monoclonal antibody (MAb) to the human insulin receptor (HIR). The HIR is localized in human brain capillary endothelium (21), which forms the BBB in vivo.

DESCRIPTION OF THE PREFERRED EMBODIMENTS

A typical BBB delivery system is the 83-14 monoclonal antibody (MAb) to the human insulin receptor (HIR). The 83-14 HIRMAb undergoes receptor-mediated transcytosis through the BBB of Old World primates, such as rhesus monkeys, but not New World primates, such as squirrel monkeys. This observation is consistent with the greater genetic similarity between humans and Old World primates, as compared to New World primates. The 83-14 HIRMAb has a very high affinity for the human or Old World primate insulin receptor and is both an endocytosing antibody in isolated human brain capillaries, and a BBB transcytosing antibody in anesthetized rhesus monkeys. The conjugation of [¹²⁵I]-bio-Aβ¹⁻⁴⁰ to the 83-14 HIRMAb is facilitated with the use of avidin-biotin technology applied to brain drug delivery. In this approach, the peptide radiopharmaceutical is monobiotinylated and, in parallel, a conjugate of streptavidin (SA) and the 83-14 HIRMAb is prepared through the formation of stable thio-ether linkage between the SA and the 83-14 MAb. The use of avidin-biotin technology applied to drug delivery takes advantage of the extremely high affinity of biotin binding ($K_D=10^{-15}$ M; dissociation $t_{1/2}=89$ days) by either avidin or streptavidin. Streptavidin is used in lieu of avidin in these studies. Owing to the cationic nature of avidin, as opposed to streptavidin, which is slightly acidic, the plasma pharmacokinetics of the MAb/SA analog is optimized as compared to the relatively rapid plasma clearance of MAb/avidin conjugates.

The invention will be better understood by reference to the following examples.

EXAMPLE 1

SYNTHESIS AND PURIFICATION OF MAB 83/14/SA CONJUGATE

The 83-14 MAb was purified from mouse ascites using protein G-Sepharose 4 Fast Flow affinity chromatography. The purified 83-14 MAb was thiolated with a 10:1 molar ratio of Traut's reagent, and Ellman's reagent was used to demonstrate that this reaction resulted in the insertion of a single thiol group on the surface of the MAb. The SA was activated with a 20:1 molar ratio of MBS, and the thiolated 83-14 MAb and the MBS-activated SA were incubated overnight at room temperature. After addition of 2 μCi of [³H]-biotin as a tracer, the sample was loaded onto a 2.3 x 92 cm column of Sephacryl S-3000 HR (Pharmacia) and eluted with 0.01 M Na₂HPO₄/0.15 M NaCl/0.05% Tween-20/pH 7.4 at 30 mL/hour for 16 hours. Fractions (3 mL) were collected and measured for A₂₈₀ and [³H] radioactivity, and this allowed for separation of the 8314/SA conjugate from the unconjugated SA, which eluted at a larger volume of the column as shown in Figures 1A and 1B.

The 8314/SA A₂₈₀ peak (Figure 1A) was greater than the 8314/SA ³H-biotin binding peak (Figure 1B), which indicated unconjugated 83-14 MAb was also contained in this peak. Owing to the very high affinity ($K_D=0.45$ nM) of the 83-14 MAb for the human BBB insulin receptor, unconjugated 83-14 MAb could compete for binding to the BBB of the 8314/SA conjugate. Therefore, unconjugated 83-14 MAb was removed by iminobiotin affinity chromatography. The fractions from the Sephacryl S-300 column were concentrated with a Centricon-30 (Amicon Inc., Beverly, MA). The iminobiotin gel (2 mL) was packed in a column (7 x 100 mm), and the column was activated with 10 mL of binding buffer (50 mM ammonium carbonate/0.5 M NaCl/pH 11.0). The 8314/SA conjugate was applied to the column followed by incubation at room temperature for 30 min, and then eluted with elution buffer (50 mM ammonium carbonate/0.5 M NaCl) of pH 4.0, 3.0 and 2.0, respectively. Only the fraction eluting at pH = 4.0 was used in subsequent studies. Fractions (0.8 mL) were collected and measured for A₂₈₀ and [³H] radioactivity as shown in Figures 1C and 1D. The number of biotin binding sites on the 8314/SA conjugate was measured with a [³H]-biotin binding assay, and was 4.0±0.2, consistent with a 1:1 conjugation of the 83-14 MAb and SA, which has 4 biotin binding sites.

EXAMPLE 2

IODINATION OF BIO-A β ¹⁴⁰ AND HYDROPHILIC INTERACTION CHROMATOGRAPHY (HILC)

Bio-A β ¹⁴⁰ (10 μ g, 2.1 nmol) was iodinated with [¹²⁵I]-iodine (2 mCi, 1.0 nmol) and chloramine T (39 nmol) at room temperature for two minutes. After addition of 125 nmol of sodium metabisulfite to quench the iodination, the reaction solution was diluted with 1 mL of 90% acetonitrile/10% 20 mM TEAP (trimethylamine/phosphoric acid)/pH 2.8 and loaded onto the PHEA extraction cartridge, which was pre-activated with 5 mL of 90% acetonitrile as shown in Figure 2. The [¹²⁵I]-bio-A β ¹⁴⁰ eluted at approximately 50% acetonitrile. These fractions were pooled and evaporated to 200 μ L. The iodinated bio-A β ¹⁴⁰ had a trichloroacetic acid (TCA) precipitation of >97% as shown in Figure 2, and was injected into the rhesus monkeys on the same day as iodination occurred.

EXAMPLE 3

GEL FILTRATION HPLC

The conjugation of [125 I]-bio-A β^{1-40} to 8314/SA was demonstrated by gel filtration HPLC using the TSK-gel G2000 SW_{IL} column. Either 0.2 μ Ci of free [125 I]-bio-A β^{1-40} or the mixture of 0.2 μ g of 8314-SA (10 pmol) was applied to the column, which was eluted with a buffer containing 0.1 M Na₂HPO₄/0.15 M NaCl/0.05% Tween-20/pH 7.0 at 0.5 mL/min for 60 min.

5 Fractions (1 mL) were collected and measured for [125 I] radioactivity. the [125 I]-bio-A β^{1-40} eluted at 12 mL, and >90% of the radioactivity shifted to an elution volume of 6-7 mL when the 8314/SA conjugate was added as shown in Figure 3 indicating >90% of the [125 I]-A β^{1-40} was biotinylated and captured by the 8314/SA conjugate.

EXAMPLE 4

10

CAPILLARY BINDING STUDIES

Human brain capillaries were isolated and cryo-preserved. The isolated capillaries were thawed at room temperature and resuspended in Ringer-Hepes buffer (RHB, pH 7.4) containing 141 mM NaCl, 4 mM KCl, 2.8 mM CaCl₂ 10 mM Hepes and 0.1% human serum albumin (HSA). The capillaries (100-125 μ g protein) were incubated with 0.025 μ Ci/ml of either [3 H]-biotin or [125 I]-bio-A β^{1-40} either in the presence or in the absence of 0.5nM of 8314/SA. Some of the tubes were enriched with 10 μ g/ml of either unconjugated 83-14 MAb or mouse IgG_{2a} for competition studies. The reaction volume was brought to 0.5 with the RHB/0.1% HSA. The incubations were performed at room temperature for 15, 30, and 60 minutes.

EXAMPLE 5

20

EMULSION AUTORADIOGRAPHY

Snap frozen AD cortex was provided by the UCLA Department of Pathology/Neuropathology, and 15 μ sections were cut on a Bright cryostat and thaw-mounted to gelatin-coated slides. The slides were warmed to room temperature, air-dried, and incubated for 30 minutes with TBM buffer (TBM = 0.05 M Tris, 0.1 % BSA, 10 mM MnCl₂, pH = 7.4). The slides were incubated with 250 μ L of TBM buffer containing 0.5 μ Ci/mL of either 125 I-bio-A β^{1-40} or 125 I-bio-A β^{1-40} /8314-SA with or without 10 μ M unlabeled A β^{1-40} for competition. The slides were incubated at room temperature for 2 hours, and were washed 4 times with 2-minute washes in 0.05 M Tris (pH = 7.4) at 4⁰C followed by two 5-second washes in H₂O at 4⁰C, and were air-dried. These slides were dipped with Kodak NTB3 emulsion in the darkroom for 5 seconds followed by air-drying at room temperature for 30 minutes, and were then put in a box and exposed at -20⁰ C in the dark. For development, the slides were removed from freezer, and thawed at room

temperature for 30 min, then fixed in 2.5% paraformaldehyde in PBS at 10°C for 30 seconds. After a PBS wash, the slides were developed with Kodak D19 developer for 2 minutes, washed in water, counterstained with methyl green-pyronine, and examined by brightfield microscopy.

EXAMPLE 6

5

PHARMACOKINETICS AND BRAIN DRUG DELIVERY

After overnight fasting, the Rhesus monkeys were sedated with an i.m. dose of ketamine (10 mg/kg), and followed by anesthesia with 1.5% halothane. A 1.0 mL volume of buffered saline (pH = 7.4) containing 300 µCi (32 µCi/kg) of either unconjugated [¹²⁵I]-bio-Aβ¹⁻⁴⁰ or [¹²⁵I]-bio-Aβ¹⁻⁴⁰ coupled to 60 µg of the 8314/SA vector was injected intravenously, and blood samples were collected at 0.25, 2.5, 5, 15, 30, 60, 120, and 180 minutes post-dose for monkey #1 (18 years) and #2 (26 years). The two monkeys were sacrificed by a lethal injection of sodium pentobarbital (100 mg/kg), and brains were removed instantly, cut into 5 coronal slabs, and frozen in powdered dry ice, and stored at -70°C for subsequent frozen sectioning and phosphorimaging. Gray and white matter of the frontal cortex were separated, and radioactivity was counted using a Beckman gamma counter. For the time-course study, the conjugate of [¹²⁵I]-bio-Aβ¹⁻⁴⁰ (300 µCi) and 8314/SA (60 µg) was injected intravenously to monkey #3 and #4 (both 15 years) after sedation with 10 mg/kg ketamine (i.m.). Monkey #3 was sacrificed 24 hours post-dose, while monkey #4 was sacrificed 48 hours post-dose for the removal of brain.

Pharmacokinetic parameters were calculated by fitting the plasma radioactivity data of monkey #1 and #2 to a biexponential equation:

$$A(t) = A_1 e^{-k_1 t} + A_2 e^{-k_2 t}$$

where A(t) = % injected dose (ID)/mL plasma. The biexponential equation was fit to TCA-precipitable plasma radioactivity data using a derivative-free non-linear regression analysis (PARBMDP, Biomedical Computer P-Series, developed at UCLA Health Sciences Computing Facilities). The data were weighted using weight = 1/(concentration)², where concentration = %ID/mL plasma. The brain volume of distribution (V_D) and the BBB permeability-surface area (PS) product of [¹²⁵I]-bio-Aβ¹⁻⁴⁰ after i.v. injection, and the pharmacokinetic parameters such as plasma clearance (Cl), initial plasma volume (V_C), systemic volume of distribution (V_{ss}), and steady state area under the plasma concentration curve $\left(AUC \Big|_0^\infty \right)$, were determined from the A₁, A₂, k₁, k₂.

30

EXAMPLE 7

PHOSPHORIMAGER ANALYSIS

Following sacrifice of the animal, the monkey brain was rapidly removed from the cranium and sectioned into 5 coronal slabs of approximately 4 mm. Each slab was individually plunged into powdered dry ice for rapid freezing over 30 minutes. Embedding medium was placed between the brain slab and circular slabs of laboratory cork (35 mm diameter, 1/8 inch thickness), and this was placed back in the powdered dry ice for additional freezing over a 2 hour period. These preparations were then stored at - 70°C in 35 mm petri dishes. For frozen sectioning, the brain was thawed to - 20°C and the cork was mounted on a cryostat orientable object holder with additional embedding medium and placed on a universal holder, and 20 µm sections were cut on a Bright cryostat at -20°C. Sections were mounted on precleaned Fisher microscope slides (75 x 50 x 1 mm) and air-dried at room temperature for 60 minutes. The slides were then glued to a paper grid, which was wrapped in transparent film, and placed in a large cassette with a 35 x 43 cm phosphorimager screen. The cassette was developed at room temperature for 45 days and the screen was read using a phosphorimager scanner (Molecular Dynamics) under high resolution mode. The images were electronically transferred as a TIFF file with Fetch-FTP for Macintosh 2.1.2. (Dartmouth College, Hanover, NH) to the laboratory Power Macintosh 7100/66 microcomputer, and were opened as PICT files in Adobe Photoshop, colorized with NIH Image software, and prints were obtained with a Pictography 3000 digital printer (Fujix, Tokyo, Japan).

EXAMPLE 8

The affinity of the 83-14 MAb for the human brain insulin receptor was unaffected by conjugation of the 50,000 Da streptavidin to the antibody, as demonstrated by the radioreceptor data shown in Figure 4. In this study [³H]-biotin was bound to the 8314-SA conjugate and incubated with human brain capillaries with or without 10 µg/mL unconjugated 83-14 MAb. The binding of the [³H]-biotin/8314-SA to the isolated human brain capillaries reached 10% at 60 minutes of incubation at room temperature as shown in Figure 4, which is comparable to the binding to human brain capillaries of unconjugated [¹²⁵I]- labeled 83-14 MAb.

EXAMPLE 9

The binder of [¹²⁵I]-bio-Aβ¹⁻⁴⁰ to human brain capillaries was tested in the presence of either no vector or the 8314-SA vector, with or without 10 µg/mL unconjugated 83-14 MAb. The results are shown in Figure 5. These results showed avid binding of the [¹²⁵I]-bio-Aβ¹⁻⁴⁰/8314-SA conjugate to the human brain capillaries that was suppressed to the background level

by the inclusion of 10 $\mu\text{g/mL}$ unconjugated 83-14 MAb. This background level is defined by the capillary uptake of [^{125}I]-bio- $\text{A}\beta^{1-40}$ without any antibody added.

EXAMPLE 10

The binding of the [^{125}I]-bio- $\text{A}\beta^{1-40}$ /8314-SA conjugate to the neuritic plaques of tissue sections of autopsy AD brain was demonstrated with the emulsion autoradiography studies shown in Figure 6. In these experiments, [^{125}I]-bio- $\text{A}\beta^{1-40}$ was applied to tissue section either in the absence or the presence of the 8314-SA conjugate. When the [^{125}I]-bio- $\text{A}\beta^{1-40}$ was applied in the tissue section in the form of the conjugate, the [^{125}I]-bio- $\text{A}\beta^{1-40}$ was preincubated for 45 minutes at room temperature with the 8314-SA conjugate prior to application to the AD brain tissue sections. Binding of the [^{125}I]-bio- $\text{A}\beta^{1-40}$ either alone or in the presence of the 8314-SA conjugate to the neuritic plaques of AD sections was abolished by co-incubation with 10 μM unlabeled $\text{A}\beta^{1-40}$.

EXAMPLE 11

The [^{125}I]-bio- $\text{A}\beta^{1-40}$ was rapidly removed from plasma following intravenous injection in the rhesus monkey as shown in Figure 7, and this rate of removal was further enhanced by conjugation of the peptide to the 8314-SA conjugate. The peptide was relatively metabolically labile as the percent of plasma radioactivity that was precipitable by trichloroacetic acid (TCA) was decreased to 40% and 25% at 180 minutes following the administration of either unconjugated [^{125}I]-bio- $\text{A}\beta^{1-40}$ or [^{125}I]-bio- $\text{A}\beta^{1-40}$ /8314-SA, respectively. The brain TCA-precipitable radioactivity at 3 hours after injection of the [^{125}I]-bio- $\text{A}\beta^{1-40}$ /OX26-SA conjugate, $82.8 \pm 0.9\%$, was much higher than the corresponding TCA-precipitable radioactivity in serum at this time point, $26.3 \pm 0.6\%$.

EXAMPLE 12

The plasma TCA-precipitable radioactivity data was subjected to a biexponential analysis to compute the pharmacokinetic parameters shown in Table 1. The frontal cortex was counted for total [^{125}I] radioactivity, and the brain volume of distribution (V_D) was computed for the $\text{A}\beta^{1-40}$ with or without conjugation to the 8314/DA vector. The gray matter BBB permeability-surface area (PS) for the free peptide or for the conjugate was computed from the brain V_D and the plasma area under the concentration curve (AUC), and was <0.25 and $1.74 \mu\text{L/min g}$, respectively.

EXAMPLE 13

The brain V_D of the $A\beta^{1-40}$ conjugated to the 8314/SA delivery system was 710-fold greater than the brain V_D of the unconjugated peptide as shown in Figure 8, and this difference is also seen in the images obtained with the phosphorimager shown in Figure 9. There is no discernible brain uptake when the peptide was administered without the brain delivery system (Figure 9, left panel).

TABLE 1-Pharmacokinetic parameters for [125 I]-bio-A β^{1-40} and [125 I]-bio-A β^{1-40} /8314/SA conjugate after an i.v. dose.

Parameter	[125 I]-bio-A β^{1-40}	[125 I]-bio-A β^{1-40} /8314-SA
A ₁ (%ID/ml)	0.137	0.150
A ₂ (%ID/ml)	0.0502	0.0183
k ₁ (min ⁻¹)	0.206	0.0948
k ₂ (min ⁻¹)	0.00649	0.00635
t _{1/2} ¹ (min)	3.37	7.31
t _{1/2} ² (min)	107	109
AUC ₀ ^{180'} (%ID min/ml)	6.00	3.54
AUC ₀ [∞] (%ID min/ml)	8.40	4.45
V _c (ml/kg)	65.0	68.5
V _{ss} (ml/kg)	207	272
C ₁ (ml/min/kg)	1.45	2.59

Parameters derived from the data in Figure 7. V_c, V_{ss}, C₁ refer to kg body weight

However, when the peptide pharmaceutical was administered conjugated to the BBB delivery system, there was robust uptake of the peptide radiopharmaceutical (Figure 9, right panel), and the differential uptake between white and gray matter tracts is clearly illuminated with the phosphorimager analysis. The peptide radiopharmaceutical conjugated to the 8314/SA delivery system was also injected into rhesus monkeys that were sacrificed at 24 and 48 hours after administration, to determine the rate of decline of the brain radioactivity following administration of the peptide radiopharmaceutical conjugated to the BBB delivery system.

EXAMPLE 14

The brain volumes of distribution in either white or gray matter at 3, 24, and 48 hours are shown in Figure 8, and the brain images at 3, 24, and 48 hours following administration of the peptide radiopharmaceutical conjugated to the BBB delivery system are shown in Figures 10A, 10B, and 10C, respectively. These experiments indicate that nearly 90% of the brain radioactivity is cleared by 48 hours after intravenous administration of the peptide radiopharmaceutical conjugated to the BBB delivery system. Plotting the brain V_D (Figure 8) on a semi-log plot versus time (hours) indicated that t_{1/2} of brain radioactivity is 16.0 hours (r=0.99).

The results of these experiments are consistent with the following conclusions. First, a peptide radiopharmaceutical may be specially formulated for BBB drug delivery, and this formulation requires (i) synthesis and purification of the 8314/SA conjugate (Figure 1), and (ii) synthesis and purification of radiolabeled monobiotinylated $A\beta^{1-40}$ using hydrophilic interaction liquid chromatography (Figure 2). Second, the bifunctionality of the 8314/SA conjugate is retained as this molecule both binds $[^{125}I]$ -bio- $A\beta^{1-40}$ (Figure 3), and binds the human brain capillary of BBB insulin receptor (Figures 4,5). Third, the biologic activity of the $[^{125}I]$ -bio- $A\beta^{1-40}$ peptide radiopharmaceutical is retained despite conjugation to the 8314/SA vector, as the complex still binds the neuritic plaques in sections of AD brain to a degree comparable to that of the unconjugated bio- $A\beta^{1-40}$ (Figure 6). Fourth, the pharmacokinetics of the peptide radiopharmaceutical (Figure 7, Table 1) demonstrate a relatively rapid decline in the plasma concentration and metabolic stability of the conjugate. Fifth, the brain uptake of the peptide radiopharmaceutical without conjugation to the BBB delivery system is negligible (Figures 8 and 9), but the brain uptake of the peptide radiopharmaceutical conjugated to the 8314/SA BBB delivery system is very high (Figures 8 and 9) and this brain uptake of radioactivity is nearly 90% cleared by 48 hours after intravenous injection (Figures 8 and 10).

The synthesis and purification of the 8314/SA vector requires a two-step procedure involving Sephacryl S-300 gel filtration (Figure 1), and iminobiotin affinity chromatography (Figure 2). The first chromatographic procedure removes unconjugated streptavidin, and the second chromatography removes unconjugated 83-14 MAb. The use of the iminobiotin affinity chromatography is a novel procedure that allows for elution of the 8314/SA conjugate from the iminobiotin column under relatively mild conditions. It is imperative to remove all unconjugated 83-14 MAb, because the affinity of this antibody for the BBB insulin receptor is extremely high with a K_D of 0.45 ± 0.10 nM (921). Therefore, the presence of any unconjugated 83-14 MAb in the formulation comprised of the 8314/SA complex would compete with binding of the 8314/SA conjugate to the BBB insulin receptor, and this would inhibit brain uptake of the conjugated peptide radiopharmaceutical. In parallel to the production of the 8314/SA conjugate, the monobiotinylated $A\beta^{1-40}$ must be iodinated and purified. The $A\beta^{1-40}$ is a relatively hydrophobic peptide, and the subsequent biotinylation and iodination further increases the hydrophobicity of this molecule, which makes it difficult to release the $[^{125}I]$ -bio- $A\beta^{1-40}$ from reverse phase surfaces. However, this problem is obviated and the percent recovery of $[^{125}I]$ -bio- $A\beta^{1-40}$ following iodination is high using hydrophilic interaction liquid chromatography (Figure 2). Similar results

were demonstrated previously following monobiotinylation and iodination of a vasoactive intestinal peptide (VIP) analog.

The multi-functionality of the amyloid imaging agent is retained following conjugation of [125 I]-bio-A β^{1-40} to the 8314/SA conjugate. The three domains are depicted in Figure 11, and include the amyloid binding domain, a linker domain, and a BBB transport domain. High affinity binding of the [125 I]-bio-A β^{1-40} /8314-SA to the BBB insulin receptor is demonstrated both in vitro with isolated brain capillaries (Figures 4 and 5) and in vivo in rhesus monkeys (Figure 9). The biotin binding properties of the 8314/SA conjugate is contained within the linker domain (Figure 11), and is demonstrated with the HPLC experiments in Figure 3, as well as the radioreceptor assays in Figures 4 and 5. The amyloid binding domain is comprised of the radio labeled A β^{1-40} . The retention of the amyloid binding properties of the peptide pharmaceutical following conjugation to the BBB delivery system is demonstrated with the emulsion autoradiography experiments using AD tissue sections (Figure 6). These results are similar to emulsion and film autoradiography experiments which demonstrate binding of [125 I]-bio-A β^{1-40} to amyloid plaques of sections of AD brain following conjugation of the peptide pharmaceutical to a conjugate of streptavidin and the OX26 MAb, which is a murine MAb to the rat transferrin receptor. In these previous experiments, the biotin linkage was attached to the ϵ -amino group of an internal lysine residue. In contrast, in the present invention utilizes an A β^{1-40} analog, in which the biotin moiety is attached to the amino terminus.

[125 I]-bio-A β^{1-40} is rapidly removed from the bloodstream, and is subjected to rapid metabolic degradation as indicated by the decrease in plasma TCA precipitability (Figure 6). Although [125 I]-bio-A β^{1-40} is rapidly removed from the bloodstream, and is subjected to rapid metabolic degradation as indicated by the decrease in plasma TCA precipitability (Figure 6). Although [125 I]-bio-A β^{1-40} is >90% bound by human albumin, this binding is relatively weak in vivo and does not inhibit the rapid clearance of [125 I]-bio-A β^{1-40} in vivo (Figure 7). The TCA-soluble [125 I] radioactivity in plasma at 1-3 hours following intravenous injection of the peptide may arise from proteolysis of the peptide with release of iodotyrosine. An alternative pathway is surface deiodination of the intact peptide possibly by ecto-enzymes on the endothelial surface of organ capillary beds. Evidence for this pathway is the observation that the systemic clearance (C1, Table 1) for the [125 I]-bio-A β^{1-40} /OX26-SA conjugate, 2.6 mL/min/kg, is approximately 4-fold greater than the systemic clearance of the unconjugated [125 I]-83-14 MAb in rhesus monkeys, 0.39-1.00 mL/min/kg. The rapid conversion of plasma radioactivity into TCA soluble metabolites

shown in Figure 7, indicates radioiodination may not be the optimal formulation for peptide radiopharmaceuticals used in the future, and alternative radiolabeling procedures might be considered. For example, chelating agents may be attached to ϵ -amino groups of internal lysines of the $A\beta^{1-40}$ peptide, which would allow for radiolabeling with indium-111 or technetium-99m.

5 Despite the relatively rapid rate of plasma clearance of the conjugated bio- $A\beta^{1-40}$ from plasma (Figure 7), and the relative reduction in the plasma AUC (Table 1), there is still robust brain uptake of the peptide radiopharmaceutical following attachment to the 8314/SA conjugate (Figures 8 and 9). There is a two-fold greater enrichment in brain uptake of the bio- $A\beta^{1-40}$ conjugated to the 8314/SA vector in gray matter versus white matter (Figures 8 and 9). This is consistent with the previous
10 observations showing a greater abundance of insulin receptor in gray matter versus white matter. This greater abundance of receptor is due to the approximately 3-4 fold greater vascular density in gray matter versus white matter as demonstrated in previous morphometric studies in rhesus monkey brain.

 There is no measurable brain uptake of the unconjugated bio- $A\beta^{1-40}$ by brain (Figures 8 and 9), which is consistent with previous studies in rats indicating lack of significant transport of $A\beta^{1-40}$
15 through the BBB in vivo. Earlier experiments reported a brain volume of distribution of unconjugated $A\beta^{1-40}$ following internal carotid artery perfusion that exceeded the brain plasma volume measured with labelled sucrose. However, these results are consistent with non-specific absorption of the $A\beta^{1-40}$ to the brain vasculature. The non-specific absorption of [125 I]bio $A\beta^{1-40}$ is further demonstrated with isolated brain capillaries in vitro as shown by the experiments in Figure 5, where the brain capillary
20 binding of [125 I]-bio- $A\beta^{1-40}$ without vector (plot designated as 'buffer' in Figure 5) is much greater than the non-specific binding of 3 H-biotin/8314-SA in the presence of 10 μ g/mL 83-14 MAb (Figure 4). The absorption of $A\beta^{1-40}$ to meningeal vascular surfaces has also been demonstrated in vivo in the rat. The non-specific absorption of the $A\beta^{1-40}$ to the luminal surface of the brain capillary endothelium following in vivo administration would not allow for imaging brain amyloid in AD. This amyloid is on
25 the brain side of the microvasculature and is separated from labelled $A\beta^{1-40}$ absorbed to the luminal surface of the brain capillary endothelium by the endothelial membranes that constitute the BBB in vivo. Since $A\beta^{1-40}$ does not cross the BBB, systemically infused [125 I] $A\beta^{1-40}$ cannot label the $A\beta$ amyloid in brain unless there is BBB disruption. However, the BBB is intact in Alzheimer's disease. Recent studies performed common carotid arterial infusion of relatively high doses (80-165 μ Ci/kg) of
30 [125 I] $A\beta^{1-40}$ into aged anesthetized squirrel monkeys. However, the only vessels labelled appeared to be meningeal vessels in brain, which are extra-cerebral vessels that lack a blood-brain barrier.

The avid brain uptake of the peptide pharmaceutical formulated as a conjugate with the BBB delivery system (Figure 9) demonstrates that brain structures can be readily imaged with this approach as the quality of the image is comparable to a standard '2-deoxyglucose' image seen with PET scans in humans or quantitative autoradiography in rats. The clear image of the distribution of the peptide radiopharmaceutical in brain (Figure 9) is due to the high activity of the 83-14 MAb as a BBB delivery sector. The PS product of BBB transport of the 83-14 MAb in the primate brain, 5.4 $\mu\text{L}/\text{min}/\text{g}$ (21), is nearly 10-fold greater than the PS product of BBB transport of an anti-transferrin receptor MAb in the primate brain. The image in Figure 9 demonstrates it is possible to achieve a high distribution of a peptide radiopharmaceutical in brain using a BBB delivery system, whereas there is negligible brain uptake of the peptide radiopharmaceutical when no BBB delivery system is used. The time course studies in Figure 10 indicate that nearly 90% of the peptide radiopharmaceutical that is initially extracted by brain is subject to metabolic transformation and clearance from brain by 48 hours after intravenous administration. However, it is anticipated that the 48 hour signal in subjects with A β amyloid will be considerably increased above the background level shown in Figure 10 for subjects that contain no brain amyloid. This is because once the peptide radiopharmaceutical traverses the BBB, the imaging agent will come in contact with extracellular amyloid, and soluble A β^{1-40} immediately deposits on the surface of pre-existing A β amyloid plaque. The A β plaque may constitute up to 15% of the brain volume in Alzheimer's disease. This deposition will effectively increase the organ residence time of the radioactivity in brain. In the absence of extracellular amyloid, the imaging agent will undergo receptor-mediated endocytosis into cells in brain bearing insulin receptor on the cell membrane surface, and this endocytosis is followed by degradation within the lysosomal compartment and release of the iodide radioactivity (Figure 10). However, the susceptibility of A β^{1-40} to protease attack is greatly reduced following deposition onto pre-existing A β amyloid.

The formulation of the amyloid imaging agent described in Figure 11 may appear to be relatively complex from the point of view of manufacturing this agent as an amyloid imaging agent for use in human subjects suspected of having Alzheimer's disease. However, the formulation of the amyloid imaging agent is simplified with the use of avidin-biotin technology, and the use of a '2-vial' formulation. One vial contains the MAb/avidin fusion protein, and the second vial contains the radiolabeled, biotinylated A β^{1-40} peptide. The two vials may be mixed immediately prior to administration to the subject, which takes advantage of the rapid capture of biotin analogs by MAb/avidin fusion proteins. Recently, an MAb/avidin fusion gene and fusion protein have been synthesized and expressed, and demonstrated to have optimal pharmacokinetics. The immunogenicity

of the MAb portion of the delivery vector may be minimized by 'humanization' of the murine framework sequences of the MAb. The immunogenicity of the avidin component may be minimized owing to oral antigen tolerance, induced by the presence of egg products in the diet. Indeed, relatively large (10 mg) quantities of avidin have been administered intravenously to humans without significant immunologic sequelae.

In summary, it has been demonstrated that peptide radiopharmaceuticals may be specially formulated to enable these molecules to undergo receptor-mediated transport through the BBB. The use of this brain drug delivery approach may allow for imaging brain amyloid or other structures using specific peptide radiopharmaceuticals that are intended to image a specialized function or property of brain.

Although the present invention has been described with reference to preferred embodiments, workers skilled in the art will recognize that changes may be made in form and detail without departing from the spirit and scope of the invention.

Abbreviations used: BBB, blood-brain barrier; SA, streptavidin; $A\beta^{1-40}$, first 40 amino acids of β -peptide of Alzheimer's disease; MAb, monoclonal antibody; HILC, hydrophilic interaction liquid chromatography; APP, amyloid peptide precursor; HIR, human insulin receptor; TEAP, triethylamine phosphate; HSA, human serum albumin; RHB, Ringer's Hepes buffer; ID, injected dose; V_D , brain volume of distribution; PS, permeability-surface area product; Cl, systemic clearance; V_c , systemic plasma volume of distribution; V_{ss} , systemic steady state volume of distribution; AUC, area under the plasma concentration curve; 8314/SA or 8314-SA, conjugate of 83-14 HIRMAb and streptavidin; K_D , dissociation constants; TCA, trichloroacetic acid; OX26, murine MAb to rat transferrin receptor; OX26/SA, conjugate of OX26 MAb and streptavidin; bio, biotinylated; bio- $A\beta^{1-40}$ /8314-SA, biotinylated $A\beta^{1-40}$ peptide coupled to a conjugate of the 83-14 MAb and streptavidin; i.v., intravenous; i.m., intra-muscular

What is claimed is:

1. A radiolabeled peptide pharmaceutical conjugated to a blood-brain barrier delivery system.

5

2. The composition of claim 1 wherein said radiolabeled peptide pharmaceutical is a radiolabeled truncated analog of $A\beta^{1-43}$, wherein $A\beta^{1-43}$ represents the 43 amino acids of the β -peptide of Alzheimer's disease.

10

3. The composition of claim 2 wherein said radiolabeled truncated analog of $A\beta^{1-43}$ is radiolabeled $A\beta^{1-40}$, wherein $A\beta^{1-40}$ represents the first 40 amino acids of the β -peptide of Alzheimer's disease.

15

4. The composition of claim 3 wherein said radiolabeled $A\beta^{1-40}$ is radiolabeled with a member selected from the group consisting of ^{125}I , ^{111}In , and $^{99\text{m}}\text{Tc}$.

5. The composition of claim 3 wherein said radiolabeled $A\beta^{1-40}$ is [^{125}I]- $A\beta^{1-40}$.

20

6. The composition of claim 1 wherein said blood-brain barrier delivery system is a vector capable of crossing the blood-brain barrier by transcytosis.

7. The composition of claim 6 wherein said vector is a monoclonal antibody to the human insulin receptor.

25

8. The composition of claim 7 wherein said monoclonal antibody to the human insulin receptor is 83-14 monoclonal antibody.

9. The composition of claim 6 wherein said vector is conjugated to said radiolabeled truncated analog of $A\beta^{1-43}$ by a polymeric linking agent.

30

10. The composition of claim 9 wherein said polymeric linking agent is polyethyleneglycol.

11. The composition of claim 10 wherein said linking agent comprises biotin and streptavidin.

12. Biotinylated $A\beta^{1-40}$ peptide coupled to a conjugate of the 83-14 monoclonal
5 antibody to the human insulin receptor and streptavidin.

13. The method for in vivo imaging of amyloid in the human brain which comprises introducing a composition comprising a radiolabeled peptide pharmaceutical conjugated to a blood-brain barrier delivery system into the bloodstream in a sufficient amount to provide
10 transport of said composition across the blood-brain barrier by transcytosis.

14. The method of claim 13 wherein said radiolabeled peptide pharmaceutical is a radiolabeled truncated analog of $A\beta^{1-43}$, wherein $A\beta^{1-43}$ represents the 43 amino acids of the β -peptide of Alzheimer's disease.

15

15. The method of claim 14 wherein said radiolabeled truncated analog of $A\beta^{1-43}$ is radiolabeled $A\beta^{1-40}$, wherein $A\beta^{1-40}$ represents the first 40 amino acids of the β -peptide of Alzheimer's disease.

20

16. The method of claim 15 wherein said radiolabeled $A\beta^{1-40}$ is radiolabeled with a member selected from the group consisting of ^{125}I , ^{111}In , and $^{99\text{m}}\text{Tc}$.

17. The method of claim 15 wherein said radiolabeled $A\beta^{1-40}$ is [^{125}I]- $A\beta^{1-40}$.

25

18. The method of claim 13 wherein said blood-brain barrier delivery system is a vector capable of crossing the blood-brain barrier by transcytosis.

19. The method of claim 18 wherein said vector is a monoclonal antibody to the human insulin receptor.

30

20. The method of claim 19 wherein said monoclonal antibody to the human insulin receptor is 83-14 monoclonal antibody.

21. The method of claim 18 wherein said vector is conjugated to said radiolabeled truncated analog of $A\beta^{1-43}$ by a polymeric linking agent.

22. The method of claim 21 wherein said polymeric linking agent is
5 polyethyleneglycol.

23. The method of claim 21 wherein said linking agent comprises biotin and streptavidin.

10 24. The method of claim 13 wherein said composition is biotinylated $A\beta^{1-40}$ peptide coupled to a conjugate of the 83-14 monoclonal antibody to the human insulin receptor and streptavidin.

1/9

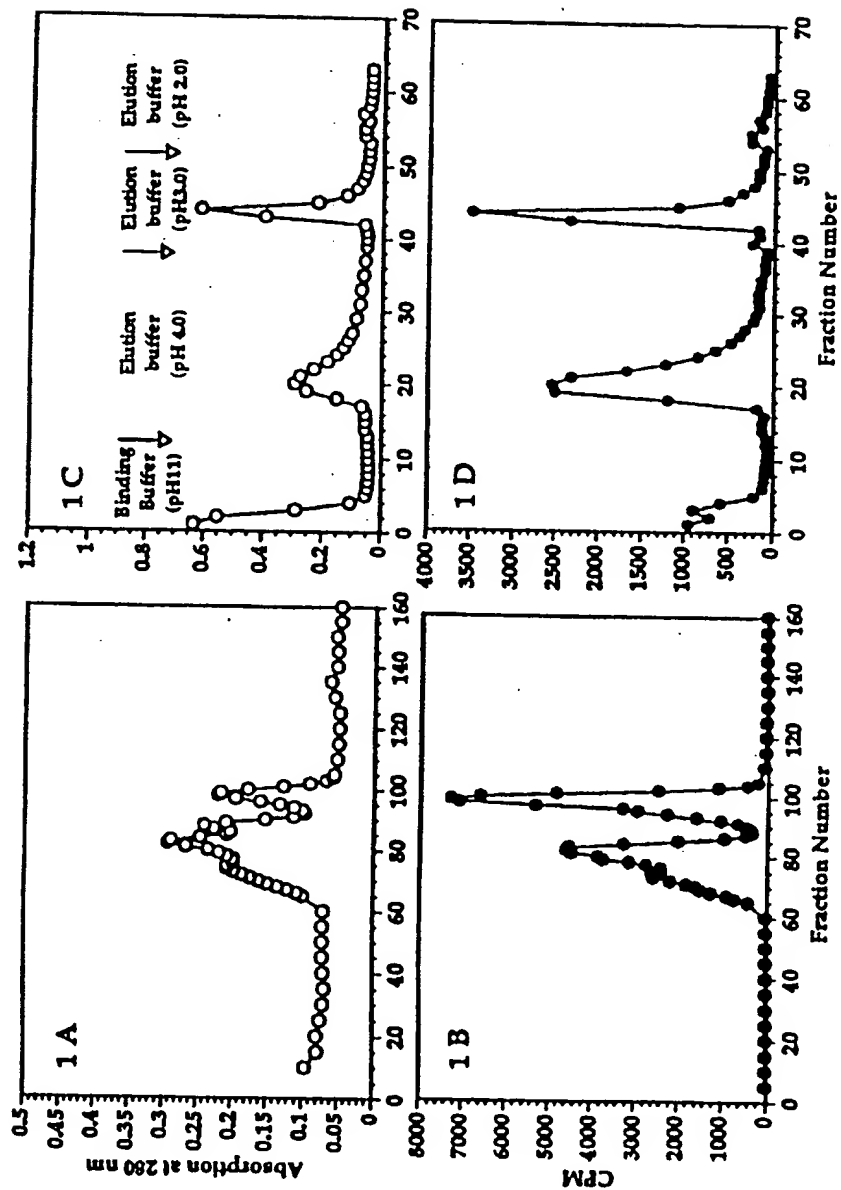


Figure 1

2/9

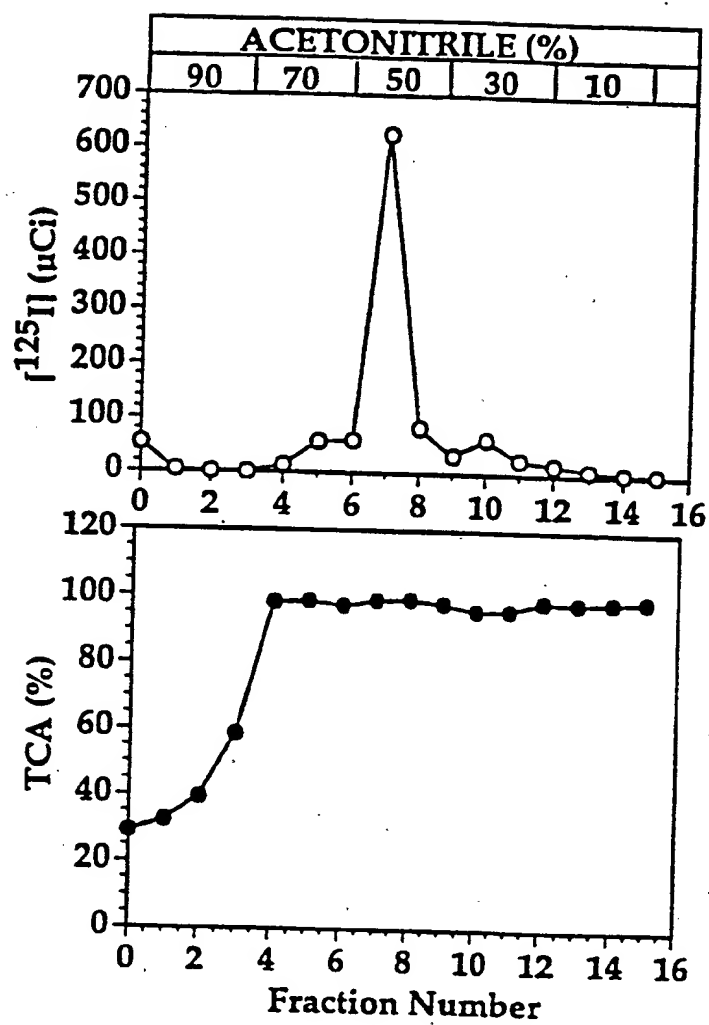


Figure 2

3/9

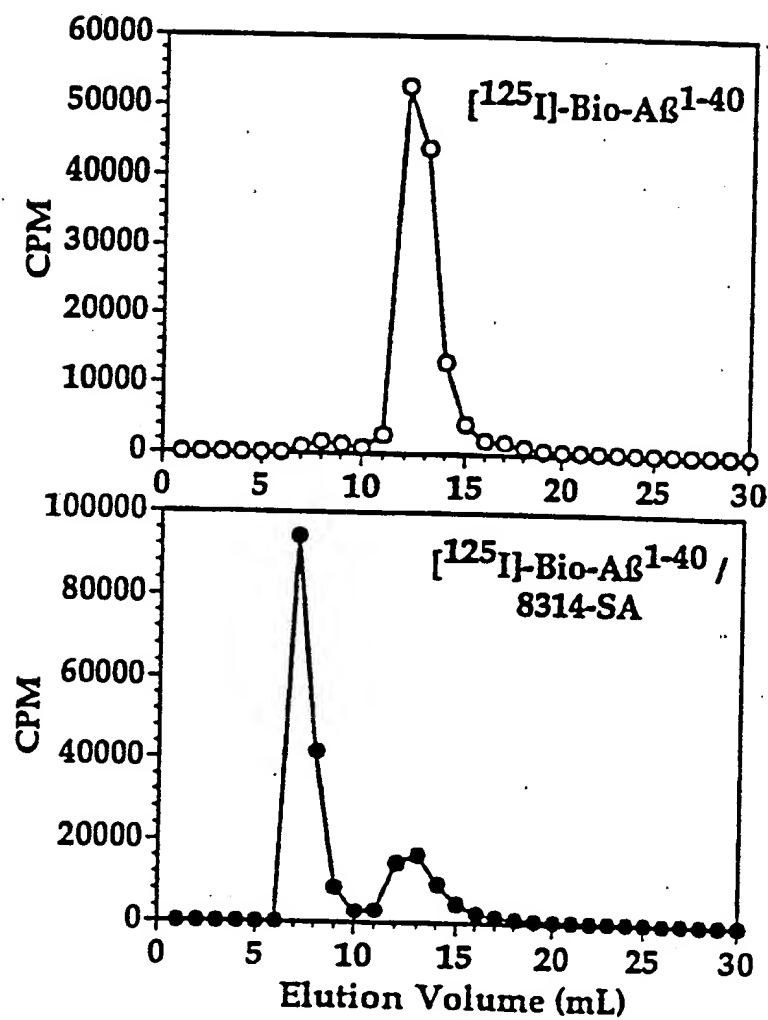


Figure 3

4/9

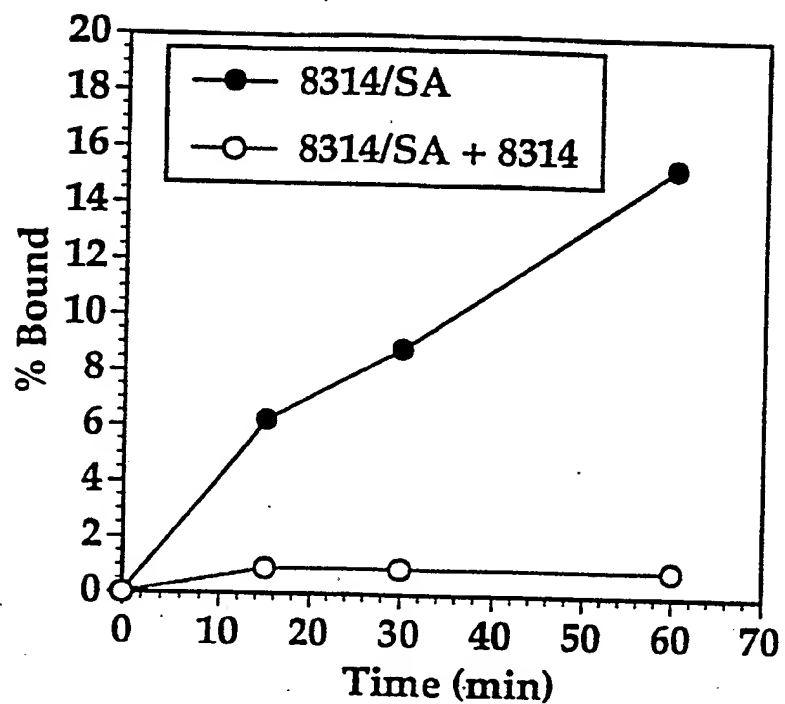


Figure 4

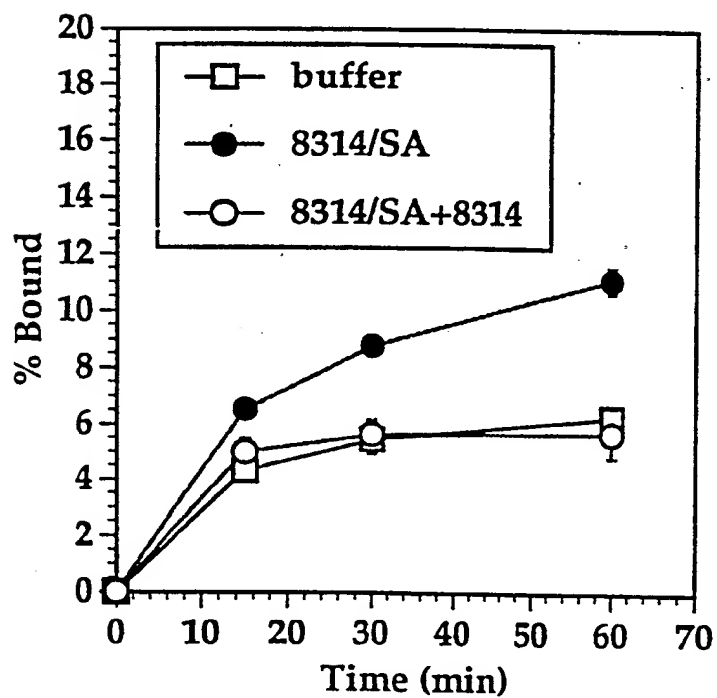


Figure 5

5/9

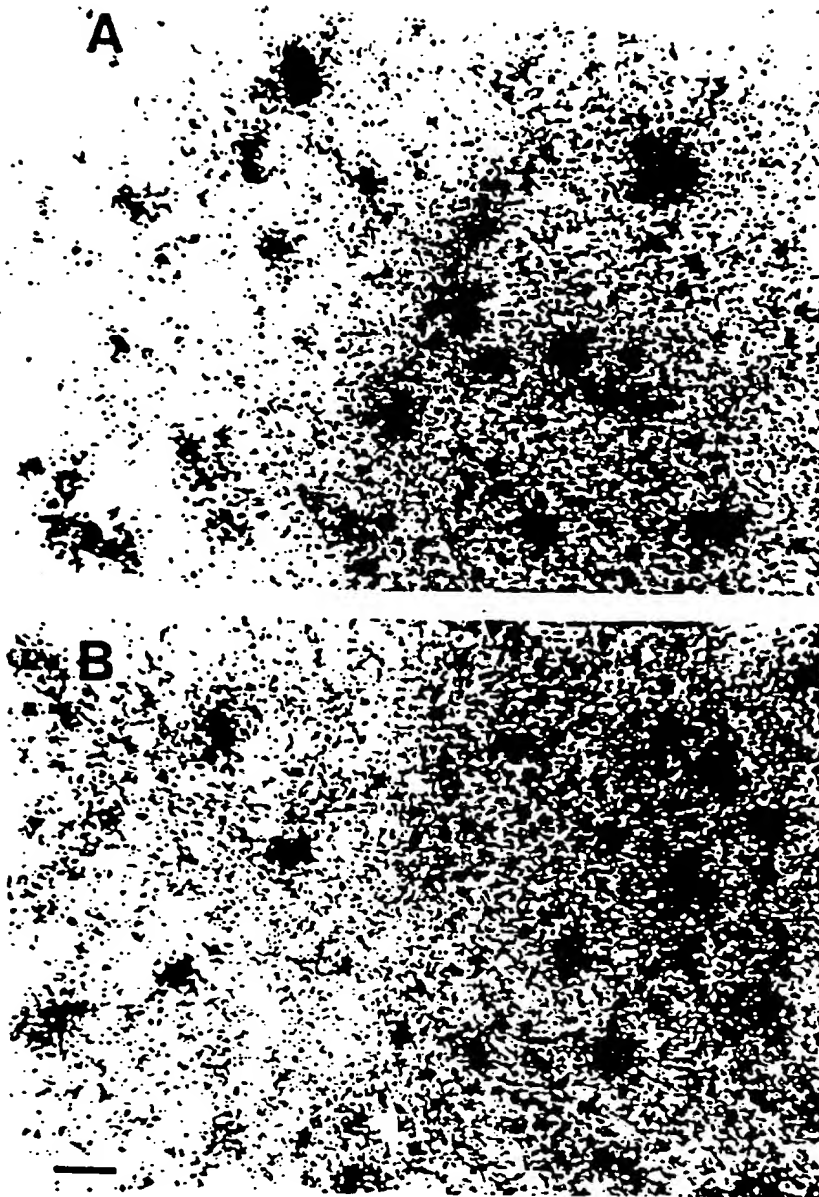


Figure 6.

6/9

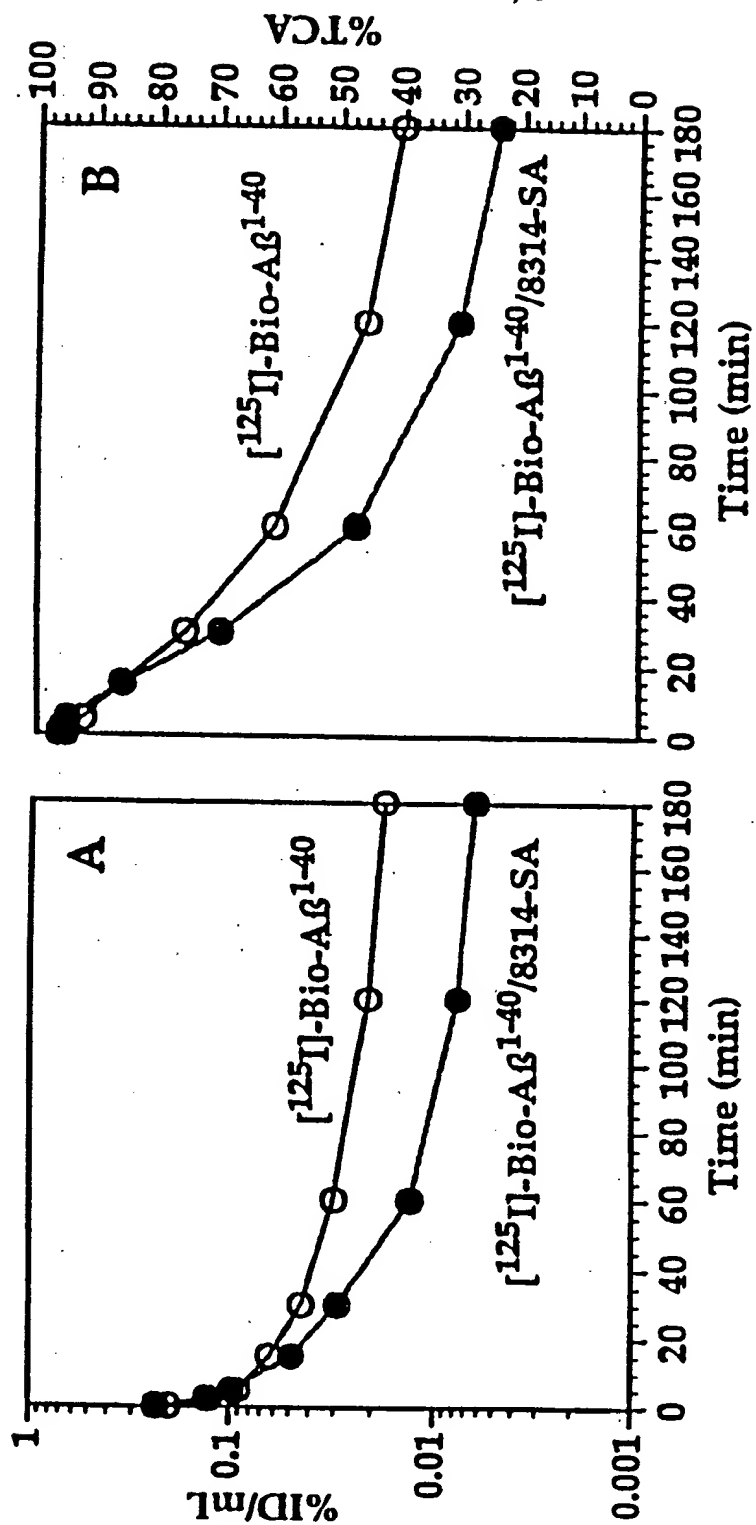


Figure 7

7/9

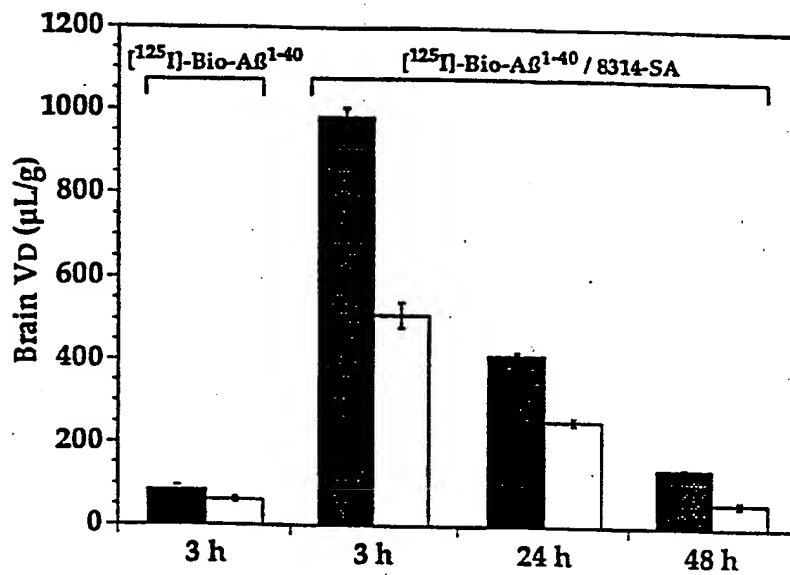


Figure 8

A left

right

B left

right



Figure 9

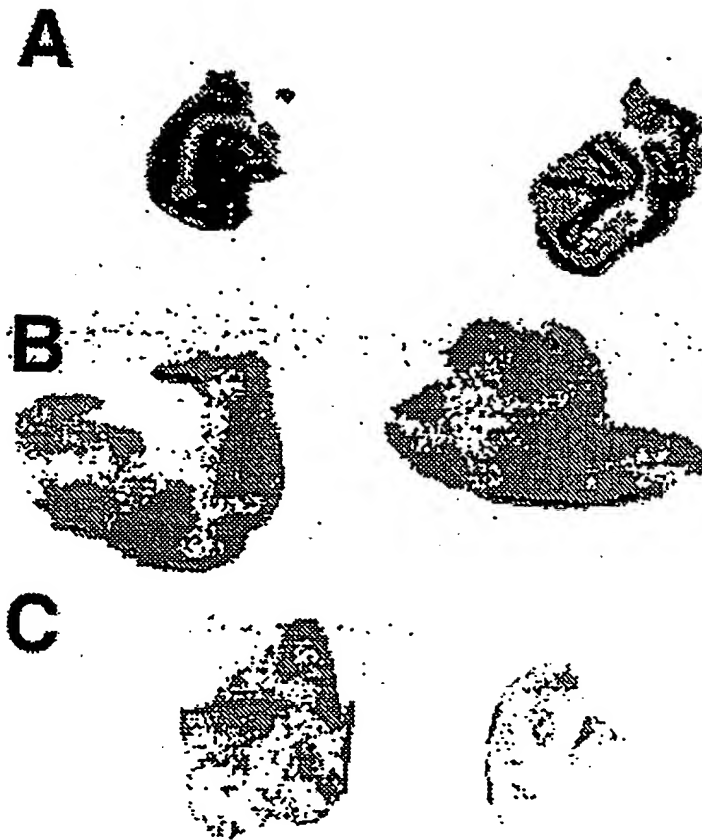


Figure 10

9/9

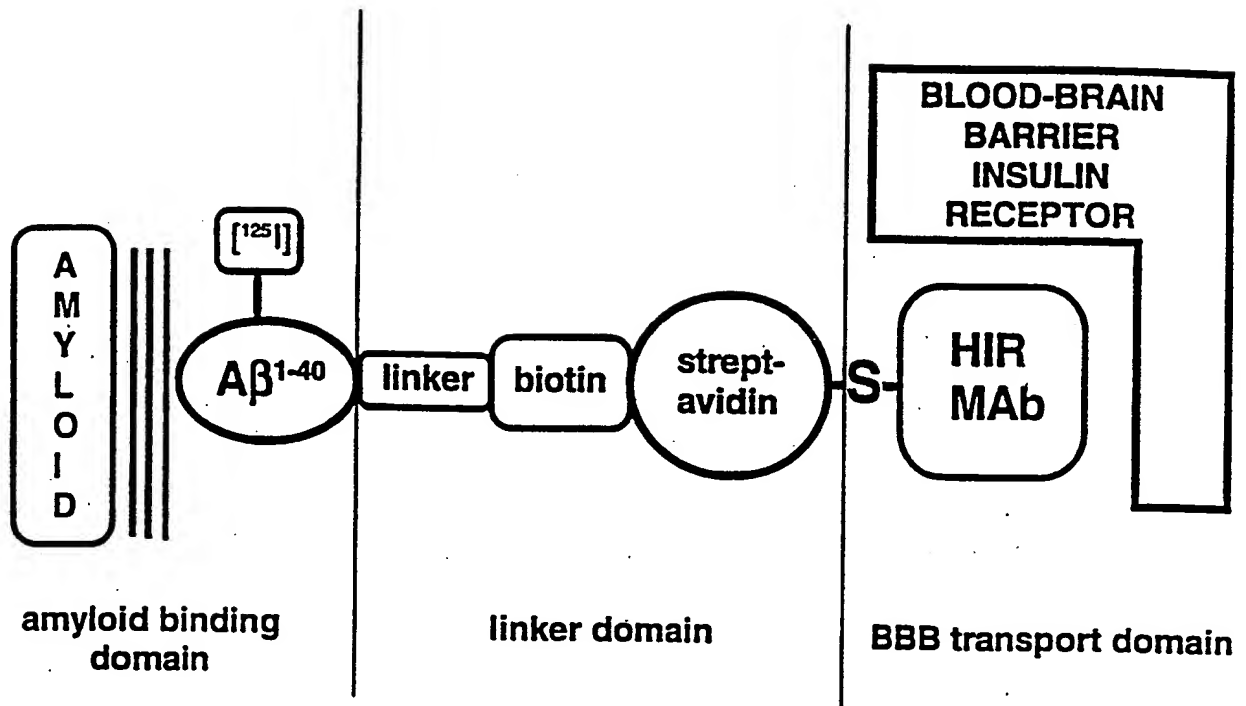


Figure 11

**This Page is Inserted by IFW Indexing and Scanning
Operations and is not part of the Official Record**

BEST AVAILABLE IMAGES

Defective images within this document are accurate representations of the original documents submitted by the applicant.

Defects in the images include but are not limited to the items checked:

- ☐ **BLACK BORDERS**
- ☐ **IMAGE CUT OFF AT TOP, BOTTOM OR SIDES**
- ☐ **FADED TEXT OR DRAWING**
- ☐ **BLURRED OR ILLEGIBLE TEXT OR DRAWING**
- ☐ **SKEWED/SLANTED IMAGES**
- ☐ **COLOR OR BLACK AND WHITE PHOTOGRAPHS**
- ☐ **GRAY SCALE DOCUMENTS**
- ☐ **LINES OR MARKS ON ORIGINAL DOCUMENT**
- ☐ **REFERENCE(S) OR EXHIBIT(S) SUBMITTED ARE POOR QUALITY**
- ☐ **OTHER:** _____

IMAGES ARE BEST AVAILABLE COPY.

As rescanning these documents will not correct the image problems checked, please do not report these problems to the IFW Image Problem Mailbox.